Auger transitions in open-shell configurations with ns ($n=4,5,6$) outer electron

H. Aksela, T. Mäkipaaso, V. Halonen, M. Pohjola, and S. Aksela
Department of Physics, University of Oulu, SF-90570 Oulu 57, Finland
(Received 24 January 1984)

Nonradiative transitions in nonclosed-shell atoms K ($Z=19$), Ag ($Z=47$), and Au ($Z=79$) with ns ($n=4,5,6$) outer electron are studied by comparing the calculated transition rates with the experimental ones. Auger transitions involving the next inner shell show clear fine structure due to the coupling of the outer ns electron with the holes producted in the Auger decay. The observed intensity distribution is found to be reproduced reasonably well with the calculations which explicitly take into account the open-shell structure.

I. INTRODUCTION

Up to now almost only closed-shell atoms (rare gases, alkaline-earth metals, Zn, Cd, Hg) have been investigated by Auger spectroscopy by carrying out detailed comparison between theoretical and experimental transition probabilities of the fine-structure lines. This is because the closed-shell atoms are less complex both experimentally and theoretically. On the contrary, in the case of the open-shell atoms, the spectra are more complex and the theory has to deal with at least three open shells.

McGuire described[1] a method which leads to explicit formulas for Auger transition rates in any nonclosed-shell atom. Applications to specific open-shell configurations can be found in the works of McGuire,[2] Chen and Crasemann,[3] and Melhorn.[4]

In this work we study the fine structure of the Auger spectra for three open-shell atoms K($Z=19$), Ag ($Z=47$), and Au ($Z=79$) with ground-state configuration $\ldots 3s^2 3p^6 4s$, $\ldots 4s^2 4p^6 4d^{10} 5s$, and $\ldots 5s^2 5p^6 5d^{10} 6s$, respectively. For these elements an accurate interpretation of the experimental Auger spectra has recently been published.[5-7] The assignment was based on the energy levels of the doubly ionized atoms known from optical spectroscopy. Thus a detailed comparison between calculated and experimental transition rates becomes possible.

In this work the actual computations are carried out with the use of the Racah algebra program MCP of Grant.[8,9] With the MCP code we calculate the angular parts of the integrals which appear in the matrix elements of the Coulomb interaction between the jj-coupled initial and final states of the Auger decay. The program allows us to work with atomic states that contain one initial inner-shell vacancy or two final-state vacancies, coupled with the outermost partially filled shell.

II. THEORY

The radiationless transition probability is given by Fermi's golden rule as

$$T=\frac{2\pi}{\hbar}\,|\langle f\,|\,V\,|\,i\rangle\,|^2\,, \tag{1}$$

where i and f denote the initial and final states of the Auger decay in any nonclosed-shell atom. $|f\rangle$ also contains the continuum electron wave function which is assumed to be normalized per unit energy range. V is the interaction potential, restricted in this work to the Coulomb interaction.

The electrons in the subshells involved in the Auger transitions are first jj coupled to give the angular momentum quantum numbers which are then jj coupled with the outer open shell to give the total angular momentum quantum numbers. The wave function of the ηth doubly ionized final state, having the total angular momentum $J'M'$, is given as a linear combination of jj-coupled wave functions. By using jj coupling between the ηth final state and the emitted Auger electron (angular momentum j,m) we obtain

$$|\,\eta j;JM\rangle^{(f)}=\sum_{\alpha} c^{J'}_{\eta\alpha}\,|\,((\alpha;J')j)JM\rangle\,. \tag{2}$$

The wave function of the νth singly ionized initial state (total angular momentum JM) is given in intermediate coupling by

$$|\,\nu;JM\rangle^{(i)}=\sum_{\beta} c^{J}_{\nu\beta}\,|\,\beta;JM\rangle\,. \tag{3}$$

In Eqs. (2) and (3) the expansion coefficients $c^{J'}_{\eta\alpha}$ and $c^{J}_{\nu\beta}$ for the doubly ionized final and singly ionized initial states can be determined by diagonalizing the Hamiltonian matrices which are given with respect to the jj-coupled wave functions. In this work the coefficients are obtained with the MCDF programs of Grant *et al.*[10]

With the wave functions (2) and (3) describing, respectively, the final and initial states, the Auger component transition probability that a singly ionized initial state $(n_1 l_1 j_1)^{-1};J$ decays into any of the doubly ionized final states $(n_2 l_2 j_2)^{-1}(n_3 l_3 j_3)^{-1};J'$ with the emission of an electron with energy ϵ, is given by

$$T_{\nu\eta}=\frac{2\pi}{\hbar}\sum_{j}\left|\sum_{\alpha}\sum_{\beta} c^{J'}_{\eta\alpha}c^{J}_{\nu\beta}\left\langle((\alpha;J')j)JM\left|\frac{e^2}{r_{12}}\right|\beta;JM\right\rangle\right|^2. \tag{4}$$

In Eq. (4) we have summed over the possible angular mo-

TABLE I. Calculated and experimental line intensities (in percents) of the $L_{2,3}M_{2,3}M_{2,3}$ transitions of potassium.

Assignment of the final state		$L_3M_{2,3}M_{2,3}$						$L_2M_{2,3}M_{2,3}$					
		Theory			Experiment			Theory			Experiment		
Term	J	Initial state Term	J	Intensity	Line in Fig. 1	Intensity		Initial state Term	J	Intensity	Line in Fig. 1	Intensity	
^2S	$\frac{1}{2}$	^3P	2	5.4	2	9.8		^3P	0	6.2	6	6.4	
		^1P	1	5.4 (10.8)				^1P	1	6.2 (12.4)			
^2D	$\frac{3}{2}$	^3P	2	2.7	7	42.6		^3P	0	19.9	14	48.9	
		^1P	1	16.6 (19.3)				^1P	1	4.9 (24.8)			
^2D	$\frac{5}{2}$	^3P	2	17.0				^3P	0	1.7			
		^1P	1	3.1 (20.1) (39.4)				^1P	1	16.8 (18.5) (43.3)			
^2P	$\frac{1}{2}$	^3P	2	0.6	9	3.8		^3P	0	1.8	15	10.0	
		^1P	1	3.8 (4.4)				^1P	1	5.2 (7.0)			
^2P	$\frac{3}{2}$	^3P	2	2.8	10	10.5		^3P	0	0.0	16	8.1	
		^1P	1	11.6 (14.4) (18.8)		(14.3)		^1P	1	5.1 (12.1)		(18.1)	
^4P	$\frac{1}{2}$	^3P	2	1.0	11	6.7		^3P	0	2.9	17	9.2	
		^1P	1	3.2 (4.2)				^1P	1	4.9 (7.8)			
^4P	$\frac{3}{2}$	^3P	2	5.7	12	8.4		^3P	0	17.4	18	10.7	
		^1P	1	3.3 (9.0)				^1P	1	2.6 (20.0) (32.1)			
^4P	$\frac{5}{2}$	^3P	2	14.8	13	18.2		^3P	0	0.0	19	6.7	
		^1P	1	3.0 (17.8) (31.0)		(33.3)		^1P	1	4.3 (4.3)		(26.6)	

TABLE II. Calculated and experimental line intensities (in percents) of the $M_{4,5}N_{4,5}N_{4,5}$ transitions of silver.

Assignment of the final state		$M_5N_{4,5}N_{4,5}$						$M_4N_{4,5}N_{4,5}$					
		Theory			Experiment			Theory			Experiment		
Term	J	Initial state Term	J	Intensity	Line in Fig. 2	Intensity		Initial state Term	J	Intensity	Line in Fig. 2	Intensity	
^2S	$\frac{1}{2}$	^3D	3	1.6	2	3.2	3.2	^3D	1	2.6	16	6.0	6.0
		^1D	2	1.6				^1D	2	2.6			
^2G	$\frac{7}{2}$	^3D	3	1.0				^3D	1	13.0			
		^1D	2	10.7				^1D	2	1.9			
^2G	$\frac{9}{2}$	^3D	3	10.4	3	29.6	37.8	^3D	1	0.5	17	37.8	
		^1D	2	7.5	4			^1D	2	11.7	18		
^2P	$\frac{1}{2}$	^3D	3	0.4				^3D	1	0.4			
		^1D	2	1.8				^1D	2	2.0			
^2P	$\frac{3}{2}$	^3D	3	0.4				^3D	1	1.9			
		^1D	2	3.9				^1D	2	3.7			
^4P	$\frac{1}{2}$	^3D	3	0.7	7	3.3	14.9	^3D	1	0.9	21	3.2	13.5
		^1D	2	1.5				^1D	2	1.7			
^2D	$\frac{3}{2}$	^3D	3	2.3	8	4.1		^3D	1	3.3	22	4.8	
		^1D	2	3.3				^1D	2	0.8			
^2D	$\frac{5}{2}$	^3D	3	4.8	9	7.5		^3D	1	0.9	23	5.5	
		^1D	2	2.6				^1D	2	3.2			
^4P	$\frac{3}{2}$	^3D	3	2.4	6	3.5	7.9	^3D	1	7.2	20	5.9	20.4
		^1D	2	0.7				^1D	2	1.0			
^4P	$\frac{5}{2}$	^3D	3	2.2	5	4.4		^3D	1	4.2	19	14.5	
		^1D	2	0.6				^1D	2	8.2			
^2F	$\frac{5}{2}$	^3D	3	2.8	10	9.5	17.3	^3D	1	0.8	24	2.5	6.7
		^1D	2	3.3				^1D	2	3.2			
^2F	$\frac{7}{2}$	^3D	3	2.4	11	7.8		^3D	1	0.1	25	4.2	
		^1D	2	6.0				^1D	2	3.7			
^4F	$\frac{3}{2}$	^3D	3	0.5	12	3.3	27.1	^3D	1	4.6	26	4.4	15.6
		^1D	2	1.9				^1D	2	1.4			
^4F	$\frac{5}{2}$	^3D	3	1.6	13	3.9		^3D	1	6.5	27	5.3	
		^1D	2	2.3				^1D	2	1.6			
^4F	$\frac{7}{2}$	^3D	3	3.4	14	8.2		^3D	1	3.1	28	4.1	
		^1D	2	4.4				^1D	2	2.1			
^4F	$\frac{9}{2}$	^3D	3	9.7	15	11.7		^3D	1	0.1	29	1.8	
		^1D	2	1.2				^1D	2	1.2			

TABLE III. Calculated and experimental line intensities (in percents) of the $N_{6,7}O_{4,5}O_{4,5}$ transitions of gold.

Assignment of the final state Term J		$N_7O_{4,5}O_{4,5}$ Initial state Term	J	Theory Intensity			Experiment Line in Fig. 3	Experiment Intensity		$N_6O_{4,5}O_{4,5}$ Initial state Term	J	Theory Intensity			Experiment Line in Fig. 3	Experiment Intensity	
^2S	$\frac{1}{2}$	^3F	4	4.3	8.7		1	8.0		^3F	2	9.3	18.6		5	19.9	
		^1F	3	4.4						^1F	3	9.3					
^2G	$\frac{9}{2}$	^3F	4	7.8	9.1		5	10.1		^3F	2	9.1	11.2		18	17.0	
		^3F	3	1.3						^1F	3	2.1					
^2G	$\frac{7}{2}$	^3F	4	0.8	8.2					^3F	2	0.0	2.5				
		^1F	3	7.4			4	8.5	20.9	^1F	3	2.5		13.5		3.0	40.7
^2P	$\frac{1}{2}$	^3F	4	1.3	5.0	13.2				^3F	2	1.7	11.0	34.9	17		
		^1F	3	3.7						^1F	3	9.3					
^2P	$\frac{3}{2}$	^3F	4	0.0	3.5	25.8	3	2.3		^3F	2	5.1	10.2		15	20.7	
		^1F	3	3.5						^1F	3	5.1					
^4P	$\frac{1}{2}$	^3F	4	2.9	6.6		9	4.7		^3F	2	0.2	1.1		22	4.1	
		^1F	3	3.7						^1F	3	0.9					
^4F	$\frac{3}{2}$	^3F	4	3.6	5.4	17.2	8	7.5	18.2	^3F	2	6.1	6.2	14.4	21	1.9	14.5
		^1F	3	1.8						^1F	3	0.1					
^4F	$\frac{5}{2}$	^3F	4	2.6	5.2		7	6.0		^3F	2	1.7	7.1		20	8.5	
		^1F	3	2.6						^1F	3	5.4					
^4P	$\frac{3}{2}$	^3F	4	2.5	4.8		6	7.1		^3F	2	4.3	6.9		19	4.3	
		^1F	3	2.3						^1F	3	2.6					
^4P	$\frac{5}{2}$	^3F	4	0.9	1.1	5.9	2	0.4	7.5	^3F	2	4.6	12.9	19.8	14	9.0	13.3
		^1F	3	0.2						^1F	3	8.3					
^2F	$\frac{5}{2}$	^3F	4	5.3	7.8		11	3.6		^3F	2	4.0	4.2		24	6.8	
		^1F	3	2.5		12.5			9.1	^1F	3	0.2		7.4			8.0
^2F	$\frac{7}{2}$	^3F	4	2.1	4.7		10	5.5		^3F	2	0.7	3.2		23	1.2	
		^1F	3	2.6						^1F	3	2.5					
^2D	$\frac{3}{2}$	^3F	4	2.0	6.8		12	8.7		^3F	2	0.3	0.6		25	0.4	
		^1F	3	4.8						^1F	3	0.3					
^2D	$\frac{5}{2}$	^3F	4	5.6	9.4		13	12.4		^3F	2	0.8	1.2		26	0.1	
		^1F	3	3.8		29.7			36.5	^1F	3	0.4		5.0			3.6
^4F	$\frac{7}{2}$	^3F	4	2.0	6.0		14	4.4		^3F	2	1.8	2.1		27	1.1	
		^1F	3	4.0						^1F	3	0.3					
^4F	$\frac{9}{2}$	^3F	4	6.0	7.5		16	11.0		^3F	2	0.3	1.1		28	2.0	
		^1F	3	1.5						^1F	3	0.8					

menta j of the Auger electron.

The matrix element of the Coulomb interaction in Eq. (4) splits into a direct part and an exchange part. The separation of the radial part from the angular part, resulting from the use of the spherical harmonics expansion of $1/r_{12}$ (rank k), enables us to reduce the direct matrix element to the form[8,9]

$$\sum_k C_k(l_1j_1,lj;l_2j_2,l_3j_3) \times R^k(n_1l_1j_1,\epsilon lj;n_2l_2j_2,n_3l_3j_3) . \quad (5)$$

For the exchange matrix elements we get an expression analogous to (5). The coefficients $C_k(l_1j_1,lj;l_2j_2,l_3j_3)$, in other words the angular parts of the integrals appearing in the matrix elements, can be expressed as a sum of terms incorporating products of fractional parentage coefficients, recoupling coefficients and reduced matrix elements. Actual computations of the angular coefficients $C_k(l_1j_1,lj;l_2j_2,l_3j_3)$ between the jj-coupled states are carried out with the computer code MCP of Grant.[8,9] The radial integrals $R^k(n_1l_1j_1,\epsilon lj;n_2l_2j_2,n_3l_3j_3)$ are obtained from the tables given by McGuire.[11–13]

III. DISCUSSION

The $L_{2,3}M_{2,3}M_{2,3}$ transitions in K, the $M_{4,5}N_{4,5}N_{4,5}$ transitions in Ag and the $N_{6,7}O_{4,5}O_{4,5}$ transitions in Au were recently measured and interpreted by our group.[5–7] In each case the final-state holes produced by the Auger decay are in the next inner shell of the atom. The outer shell consists of one s electron. The coupling of the initial and final states of the decay with the outer s electron splits the spectrum to several fine-structure lines. The splitting due to the coupling in the final state was resolved experimentally and comparison with optically determined energy levels resulted in a detailed interpretation of the measured fine structure.[5–7] The fit of the spectrum produced relative intensity values which now can be compared with the calculations.

The experimental and calculated results are shown in Tables I–III for K, Ag, and Au, respectively. The LS term symbols given in Tables I–III lose their meaning and only J's are good quantum numbers in passing to the higher atomic numbers or from the final to the initial state. The LS term symbols are thus only of a notational value.

Owing to a very small energy separation between the electrostatic split levels of the initial state they have not been resolved experimentally. Some of the final-state levels also lie so close to each other that only the sum intensity of the corresponding line components is a reliable experimental quantity. If we compare the sum intensities, the calculated and experimental results seem to be in a reasonably good agreement with each other. For example, there is a significant discrepancy between theory and experiment in the case of the lines 15 and 17 in Table III. However, the lines 14 and 15 and the lines 16, 17, and 18 are very close together. For the sums of these lines there is fair (14+15) to excellent agreement (16+17+18) between calculation and experiment. The experimental relative intensities of the above-mentioned individual components should not be taken too literally because only the total intensities of these lines are well reproducible in the fitting procedure. This arises mainly from the difficulties in determining accurately the actual shape of the standard line.

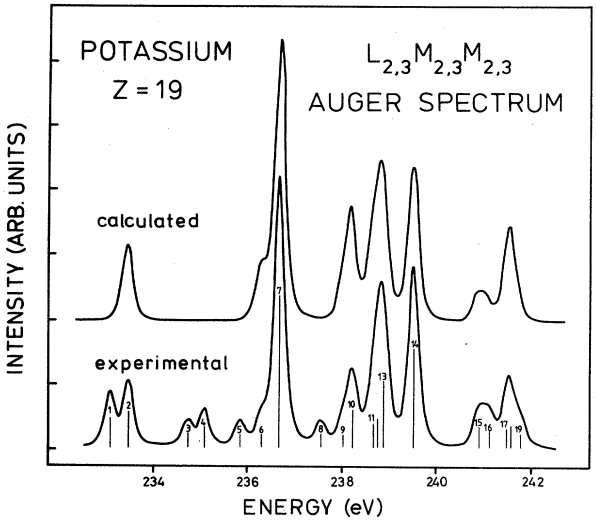

FIG. 1. $L_{2,3}M_{2,3}M_{2,3}$ spectrum of K. The lower curve shows the experimental spectrum and the upper curve the calculated profile produced by using the calculated transition rates with the experimental energies and line shapes.

The overall agreement between experiment and theory is also nicely demonstrated in Figs. 1–3, where the experimental spectra are shown together with the profiles produced by using the calculated transition probabilities with the experimental energies and line shapes. The purpose of the Figs. 1–3 is thus to give a visual display from the

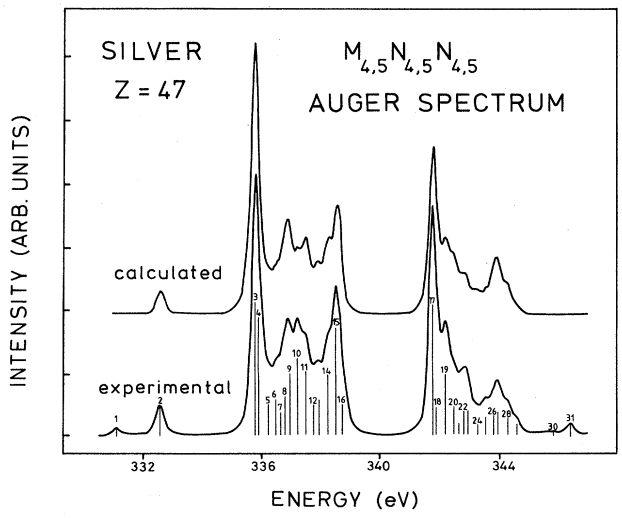

FIG. 2. Comparison between calculated and experimental intensities of the $M_{4,5}N_{4,5}N_{4,5}$ transition of Ag.

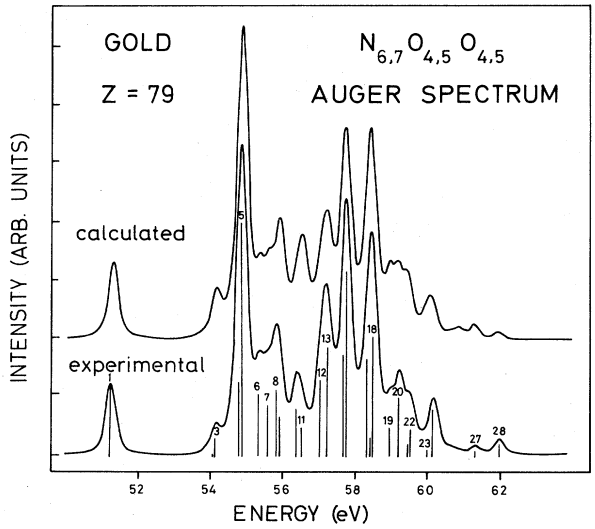

FIG. 3. Comparison between calculated and experimental intensities of the $N_{6,7}O_{4,5}O_{4,5}$ transition of Au.

comparison between experimental and calculated intensities.

Some of the lines observed in the experimental spectra are due to the Auger transitions not described by the single-configuration approach. Because such lines are ignored in the calculations, the experimental spectra contain some weak lines not presented in the calculated profiles. The description $\ldots 2p^5 3s^2 3p^6 4s \rightarrow \ldots 2p^6 3s^2 3p^4 4s$, used for potassium in the present calculations (Fig. 1) is obviously insufficient, for example. The description $\ldots 2p^5 3s^2 3p^6 (4s+3d) \rightarrow \ldots 2p^6 3s^2 3p^4 (4s+3d)$, leading to energy shifts and redistribution of the intensity, may agree better with experiment. This may be a reason for the discrepancy between present calculation and experiment in the case of the line 18 in Table I. Another reason may be the inaccurate fitting of the experimental spectrum.

The correlation effects in the spectra of open-shell atoms will be discussed in more detail in a future paper. A detailed study of the relativistic effects on the fine structure of the Auger spectra is also in progress. In this work we have presented our first detailed results for the open-shell Auger transitions in atoms with outer s electron. Reasonably good agreement between experiment and calculation is obtained.

ACKNOWLEDGMENT

This work has been supported by the Finnish Academy for Science.

[1]E. J. McGuire, in *Ionization and Transition Probabilities,* edited by B. Craseman (Academic, New York, 1975), Vol. 1, p. 293.
[2]E. J. McGuire, Phys. Rev. A **11**, 1889 (1975); **17**, 182 (1978).
[3]M. H. Chen and B. Crasemann, Phys. Rev. A **10**, 2232 (1974); **16**, 1495 (1977).
[4]W. Menzel and W. Mehlhorn, in *Inner-Shell and X-Ray Physics of Atoms and Solids,* edited by D. J. Fabian, H. Kleinpoppen, and L. M. Watson (Plenum, New York, 1981).
[5]S. Aksela, M. Kallokumpu, H. Askela, and J. Väyrynen, Phys. Rev. A **23**, 2374 (1981).
[6]J. Väyrynen, S. Aksela, M. Kellokumpu, and H. Aksela, Phys. Rev. A **22**, 1610 (1980).
[7]S. Aksela, M. Harkoma, M. Pohjola, and H. Askela (unpublished).
[8]I. P. Grant, Comput. Phys. Commun. **5**, 263 (1973).
[9]I. P. Grant, Comput. Phys. Commun. **11**, 397 (1976).
[10]I. P. Grant, B. J. McKenzie, P. H. Norrington, D. F. Mayers, and N. C. Pyper, Comput. Phys. Commun. **21**, 207 (1980); **21**, 207 (1980).
[11]E. J. McGuire, Sandia Research Laboratories Research Report No. SC-RR-71-0075 (1971) (unpublished).
[12]E. J. McGuire, Sandia Research Laboratories Research Report No. SC-RR-71-0835 (1972) (unpublished).
[13]E. J. McGuire, Sandia Research Laboratories Research Report No. SAND-75-0443 (1975) (unpublished).